# Numerical Simulation of Electroosmotic Flow in Micro Channels with Analytical Integration of Surface Potential

Zhijian Chen, Mahesh Athavale, Andrzej Przekwas
zjc@cfdrc.com, (256)726-4978, Fax: (256)726-4806
CFD Research Corporation, 215 Wynn Drive, Huntsville, AL 35805

## Abstract

We have developed a new integration methodology to simulate electroosmotic flows in micro channels, which allows us to accurately account for the effects of the double layer without resolving it. The method is a sub-grid type model that allows computational cells much larger than the thickness of double layer near the wall. This methodology is extremely suitable for incorporation into numerical flow codes, and capable of providing accurate and robust solutions to electroosmotic and electrophoretic flows in simple and complex geometries

**Keyword:** Electro osmosis, Double layer, Integration Method

## Introduction

Numerical simulation of electroosmotic flows in micro channels is complicated by the relative sizes of the double layer (10 to 100 nm) and channel width (upto 100's of μm), which makes it difficult to fully resolve the double layer. Two main approaches have been used previously: (1) applying a slip-wall velocity at the channel walls [e.g. Refs. 1,2] and (2) using a larger thickness of double layer that allows resolution of the double layer [3]. Since the typical thickness of the double layer is extremely small compared to the channel width, it would be computationally very costly to capture the velocity profile inside the double layer by placing sufficient number of grid cells in the layer to resolve the velocity changes, especially in complex, 3-d geometries. Using a larger double layer thickness (approach 2) alleviates some of these problems; however, this approach actually changes the behavior of electroosmotic flow from a "near-plug flow" to "boundary-layer flow" by increasing the double-layer thickness. The approach based on slip-walls does allow for the plug-flow nature of the flow by directly applying the electroosmotic velocity wall. This approach, however, is difficult to use when the flow geometry is complicated, e.g. flow in a T-junction, X-junction, etc. In order to overcome the difficulties arising from those two approaches, we have developed a sub-grid integration method to properly account for the physics of the double layer. Our integration approach can be used on simple or complicated flow geometries. Resolution of the double layer is not needed in this approach, and the effects of the double layer are accurately accounted for at the same time. With this approach, the numeric grid size can be much larger than the thickness of double layer. Presented in this paper are a description of the approach, methodology for implementation and several validation and demonstration simulations of electro-osmotic flows.

## Numerical Methodology

To enable simulations without resolving the double layer, its effects on the flow can be modeled using the concept of a $\zeta$ potential near the wall. A body force term, resulting from the interaction of the $\zeta$ potential and the applied electric field, is added to the fluid momentum equations, written as [3]:

$$\frac{\partial \rho u_i}{\partial t}+\frac{\partial}{\partial x_j}\rho u_j u_i=-\frac{\partial p}{\partial x_i}+\frac{\partial \tau_{i,j}}{\partial x_j}+\varepsilon\kappa^2\zeta\nabla\phi \quad (1)$$

Where, $\rho$ is the fluid density, $u_i$ the Cartesian velocity components, p the pressure, $\tau_{i,j}$ the stress tensor, $\varepsilon$ the fluid permittivity, $\delta=1/\kappa$ the Debye thickness of the double layer, and $\phi$ the applied electric potential. The $\zeta$ potential is governed by:

$$\nabla^2\zeta=\kappa^2\zeta$$

with BCs:

$$\begin{cases}\zeta=\zeta_0, & y=0\\ \zeta=0, & y=\infty\end{cases} \quad (2)$$

$\zeta$ potential decays very quickly inside the double layer: Fig. 1 shows a typical distribution of $\zeta$ potential along the wall normal direction.

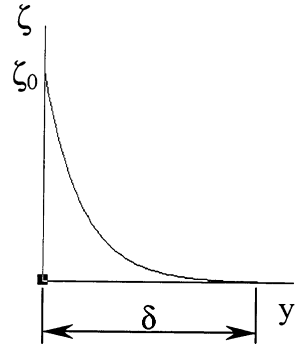


*Figure 1. The Change of $\zeta$ Potential Normal to the Wall.*

Considering the nature of $\zeta$ potential, we analytically integrate the equation (2) combining with the boundary conditions, along a local wall normal direction to obtain the distribution:

$$\varsigma=\varsigma_0 e^{-\kappa y} \quad (3)$$

Where, y is normal distance to the wall, and $\zeta_0$ is the value of $\zeta$ potential at the wall. The electroosmotic source term defined in equation (1) is only applied in a very narrow region near the wall. We also analytically integrate it while neglecting the impact of $\zeta$ potential outside the double layer:

$$\begin{aligned}\bar{S}&=\int_V \varepsilon\kappa^2\zeta\nabla\phi\cdot dV=\int_0^\delta \varepsilon\kappa^2\zeta\nabla\phi\cdot A dy=\\ &\varepsilon\kappa^2\nabla\phi A\int_0^\delta \varsigma_0 e^{-\kappa y}dy=\varepsilon\kappa\nabla\phi\varsigma_0(1-e^{-1})A\end{aligned} \quad (4)$$

Where, V is grid volume near the wall, A is the area of the wall face, and e is the Euler constant. The vector S denotes the momentum source contributions due to the applied electric fields in different directions. The shear stress on the wall is calculated as

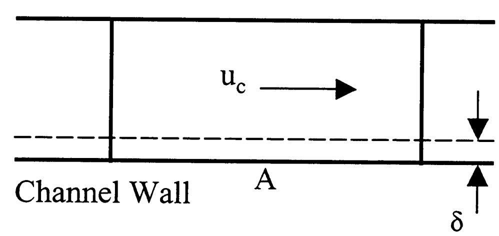


*Figure 2. Integration Grid Volume.*

$$\bar{\tau}_w=-\int_0^\delta \varepsilon\kappa^2\varsigma\nabla\phi\cdot dy \quad (5)$$

This results into

$$\bar{\tau}_w=-\frac{\varepsilon\nabla\phi\varsigma_0}{\frac{e}{e-1}\delta} \quad (6)$$

Where we used the relation $\delta=\frac{1}{\kappa}$.

In the numerical calculations, the velocity gradient at the wall is needed to calculate the shear stress. Using the plug flow arguments, the most obvious shear stress expression becomes (see Figure 2)

$$\bar{\tau}_w = -\frac{\mu(u_c - u_w)}{\delta} \qquad (7)$$

. However, a comparison with the expression in Eqn. 6 indicates that this expression needs to be modified to ensure the correct velocity gradient at the wall. Thus we decrease the effective distance to $\frac{e}{e-1}\delta$ and rewrite Eqn. 7 for the shear stress as:

$$\bar{\tau}_w = -\mu \frac{\vec{u}_c - \vec{u}_w}{\frac{e}{e-1}\delta} \qquad (8)$$

Where, $u_c$ is cell center velocity of grid near the wall and $u_w$ is the wall velocity. The wall velocity is zero for a stationary wall. This definition of the effective distance essentially reduces the apparent wall shear stress, calculated based on the available information during calculations (i.e. $u_c$, $u_w$ and $\delta$)

This approach thus fully accounts for double-layer physics, which allows its use on simple as well as complex geometries (e.g. T-junction, X-junction) where the alternative approach of slip-wall velocities can face difficulties.

## Verification and Demonstration Simulations

### *2D Straight Channel*

First case presented here involves electro-osmotic flow in a micro channel. The channel is 200-$\mu$m long and 20 $\mu$m wide. The electric potentials at left and right ends are 1 Volt and 0 Volt respectively, the relative permittivity is 78.4, the wall $\zeta$ potential $\zeta_0$ = -1 Volt, and double layer thickness, $\delta$, is 10 nm. Figure 3 shows the computational geometry and boundary conditions. Figure 4 shows the computed velocity vectors; it is clearly a plug type flow as anticipated. Table 1 gives a comparison of the calculated and analytical values of the bulk axial velocity, which are in excellent agreement.

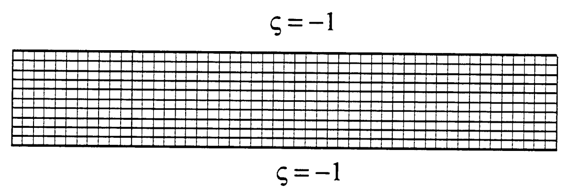


*Figure 3. Straight Micro Channel and Boundary Conditions.*

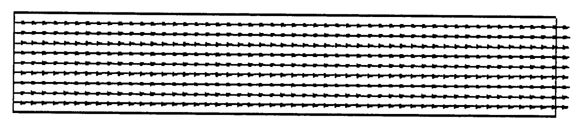

*Figure 4. Calculated Velocity Vectors.*

**Table 1: Comparison of Fluid Velocity outside the Double Layer**

| | |
|---|---|
| Analytical Solution | $3.469\times10^{-3}$ m/s |
| Numerical Solution | $3.471\times10^{-3}$ m/s |
| Error | 0.057% |

### *3D Cross Channel*

The second test case presented here is the flow in a 3-d, cross-shaped channel. Figure 5 shows the channel configuration. The channel width h is 30 $\mu$m, the channel aspect ratios L/h and W/h are 6.33 and 5 respectively and the channel depth is 10 $\mu$m, the double layer thickness $\delta$ is set to 10 nm, the applied potential at the left and right ends 1 and 2 are 1 Volt and 0 Volt, respectively, and the top and bottom ends (3 and 4) are set to no electric flux conditions, the front and back surface along the depth of channel are symmetry boundaries. Figure 6 and 7 show the velocity vectors and electric potential, respectively, in the center cutting plane.

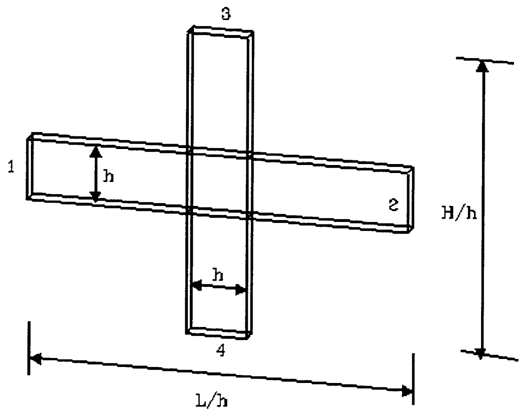


*Figure 5. 3D Cross Channel Geometry.*

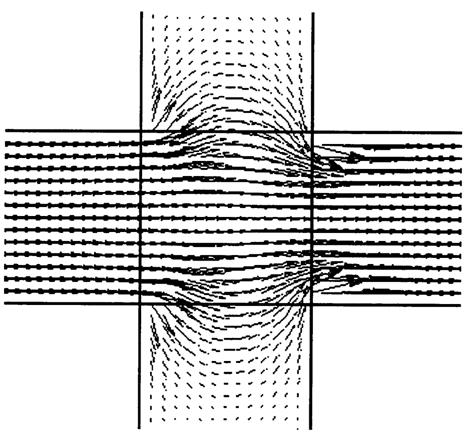

*Figure 6. Velocity Vectors at Channel Cross Section.*

We can see that the characteristic "plug flow" can be captured using our integration method even for this complicated geometry, and where the cell sizes next to the walls are much larger than the thickness of double layer.

## Conclusions

A new integration methodology has been developed to handle electroosmotic flows. This method allows the use of relatively large sized computational cells near the walls and properly accounts for the physics of the extremely thin double layer without having to resolve the velocity distribution in the double layer. This methodology thus can provide an effective means for numerical simulations of electroosmotic flows in simple as well as complex flow geometries. The formulation also avoids the explicit use of slip velocities at channel walls. Two sample examples shown here demonstrate the capabilities of the method; it has also been applied successfully to a variety of other flow problems with more complex flow geometries as well as to problems dealing with electrophoresis.

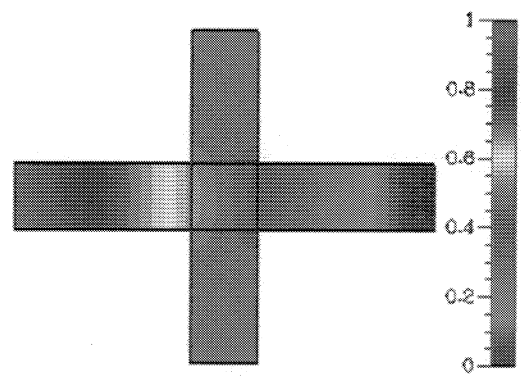


*Figure 7. Electric Potential inside Channel.*

## References

[1] Patankar, N.A., and Hu, H.H., "Numerical Simulation of Electroosmotic Flow," *Anal. Chem.*, 70, 1998, pp. 1870-1881.

[2] Krishnammorthy, S., and Giridharan, M.G., "Analysis of Sample Injection and Band-Broadening in Capillary Electrophoresis Microchips," MSM Technical Proceedings, 2000.

[3] David Erickson, D., Li, D., "Influence of Surface Heterogeneity on Electro kinetically Driven Micro Fluidic Mixing," Langmuir, 2002, 18, pp1883-1892.